Effects of bursty traffic in service differentiated Optical Packet Switched networks

Harald Øverby, Norvald Stol

Department of Telematics, Norwegian University of Science and Technology,
O.S. Bragstadsplass 2E, N-7491 Trondheim, Norway
haraldov@item.ntnu.no

Abstract: Service differentiation is a crucial issue in the next-generation Optical Packet Switched networks. In this paper we examine how bursty traffic influences the performance of a service differentiated Optical Packet Switched network. By using time-continuous Markov chains, we derive explicit results for the packet loss rates in the case of a bursty hyper-exponential arrival process. Results indicate that the performance is degraded as the burstiness of the arrival process increases.

©2004 Optical Society of America

OCIS codes: (060.4250) Networks; (060.4510) Optical Communications

References and links

1. M. O'Mahony, D. Simeonidou, D. Hunter and A. Tzanakaki, "The Application of Optical Packet Switching in Future Communication Networks," IEEE Communications Magazine **39**, 128-135 (2001).
2. X. Xiao and L. M. Ni, "Internet QoS: A Big Picture," IEEE Network **13**, 8-18 (1999).
3. B. Wydrowski and M. Zukerman, "QoS in Best-Effort Networks," IEEE Communications Magazine **40**, 44-49 (2002).
4. M. Yoo, C. Qiao and S. Dixit, "QoS Performance of Optical Burst Switching in IP-Over-WDM Networks," IEEE Journal on Selected Areas in Communications **18**, 2062-2071 (2000).
5. H. Øverby and N. Stol, "A Teletraffic Model for Service Differentiation in OPS networks," *in Proceedings of IEEE 8th Optoelectronics and Communications Conference* (Institute of Electrical and Electronic Engineers, 2003), pp. 677-678.
6. Ayman Kaheel, Tamer Khattab, Amr Mohamed and Hussein Alnuweiri, "Quality-of-Service Mechanisms in IP-over WDM Networks," IEEE Communications Magazine **40**, 38-43 (2002).
7. W. Leland, M. Taqqu, W. Willinger and D. Wilson, "On the Self Similar Nature of Ethernet Traffic (Extended Version)," IEEE/ACM Transactions on Networking **2**, 1-15 (1994).
8. A.L. Schmid et al., "Impact of VC merging on buffer requirements in ATM networks," Proceedings of Eighth International Conference on High Performance Networking, 203-217 (1998).
9. Deepankar Medhi, "Some Results for Renewal Arrival to a Communication Link," Probability Models and Statistics: A J. Medhi Festschrift, 85-107 (1996).
10. S. Bjørnstad, N. Stol and D. R. Hjelme, "Quality of service in optical packet switched DWDM transport networks," *in Asia-Pacific Optical and Wireless Communications Conference*, Proc. SPIE **4910**, 63-74 (2002).
11. E. V. Breusegem, J. Cheyns, B. Lannoo, A. Ackaert, M. Pickavet and P. Demeester, "Implications of using offsets in all-optical packet switched networks," *in Proceedings of IEEE Optical Network Design and Modelling* (Institute of Electrical and Electronic Engineers, 2002).
12. Leonard Kleinrock, *Queueing Systems Volume I: Theory* (John Wiley & Sons, 1975).

1. Introduction

In order to increase available capacity in future core networks, Wavelength Division Multiplexing (WDM) has emerged as a viable technology [1]. Among the different WDM switching technologies proposed in recent literature, Optical Packet Switching (OPS) has emerged as the most promising, at least in the long run, due to the benefits from statistical multiplexing and adaptability to changes in the network infrastructure and traffic pattern [1].

Today's Internet provides only the best-effort service, where each packet is getting the same treatment and there are no guarantees to the end-to-end delay or the packet loss rate

(PLR) [2]. However, the increasing number of real-time applications and interactive Internet applications demand a stricter Quality of Service (QoS) than the current best-effort service can offer. Although the best-effort service is not suited to carry real-time or interactive applications, it is well suited for web browsing, e-mail and other relaxed services. Hence, in order to give different applications their needed level of QoS and to utilize network resources optimally, service differentiation should be present in future core networks [2].

Existing service differentiation schemes for traditional store-and-forward networks mandate the use of electronic buffers to isolate the different traffic classes, i.e. by the use of active queue management algorithms [3]. Here, all packet arrivals to a switch are stored in the buffer and managed according to an active queue management algorithm, which isolate the different service classes by marking, dropping or reordering packets in the queue [3]. However, as pointed out in [4], such schemes are not suitable for the WDM layer. First, electronic buffering necessitates the use of optical-electrical converters, which results inn a significant increase in the cost of the switch. Second, although optical buffering can be realized by utilizing Fibre Delay Lines (FDLs), they can only give limited buffering capabilities compared to electronic buffering, because data is delayed by traversing a fixed length optical fibre (i.e. the FDL is not a Random Access Memory). Hence, performing active queue management on FDL buffers is not an easy task, as complex management is required. Also, using FDLs makes the switches bulky and costly, especially when large amounts of data need to be buffered. Hence, as pointed out in [4], a viable service differentiation scheme for future optical core networks is to utilize bufferless methods to isolate the different service classes. One such bufferless method is the Wavelength Allocation algorithm (WA) [5,6].

According to [7], the Internet traffic shows a self-similar pattern, which means that the traffic is equally bursty when viewed over different time scales. Regarding arrivals to an optical switch, this results in periods with many arrivals and periods with little or no arrivals. The widely used Poisson process does not model such traffic very well, which means that other arrival processes should be considered, e.g. the hyper-exponential arrival process [8,9].

In earlier works we have presented an analytical model of the WA in the case of a non-bursty Poisson arrival process [5]. This paper presents an analytical model of the WA in the case of a bursty hyper-exponential arrival process and further considers the impacts of bursty traffic on the network performance. The rest of the paper is organized as follows. Section 2 presents the system model. Section 3 presents the WA, accompanied by analytical models. Section 4 presents simulation and analytical results, while Section 5 concludes the paper.

2. System model

We consider a network with two service classes, where service class 0 is given higher priority than service class 1 (the use of two service classes only in the core networks is argued by the authors of [10]). Since the switches in the network have no buffers for contention resolution, the aggregated delay will be very small compared to the delay from the access network, and can thus be ignored [10]. However, a major concern is such networks is packet losses, which is caused by external blocking (i.e. contentions at an output port). Hence, in this paper we focus on the PLR as the sole QoS parameter, which means that the different service classes will be isolated from each other based on different PLRs. When a packet arrives at the switch, the packet header is extracted and processed electronically by the control module. While the header is processed, the packet payload is buffered using FDL processing buffers (as seen in Fig. 1(a) [11]. Based on the destination information extracted from the packet header, the control module decides which output fibre the packet is switched to and configures the switch fabric accordingly. For the rest of the paper we focus on a single optical core switch and assume the following:

- The optical switch operates in asynchronous mode.
- The switch utilizes full wavelength conversion.
- The switch has F input- and output fibres, as shown in Fig. 1(a).

- By utilizing WDM, each fibre provides N wavelengths (channels) to transport data, each wavelength with a specified capacity C bps.
- We assume a uniform traffic pattern, which means that we have an equal load on every output fibre and can restrict our study to consider the PLR on a single output fibre, marked red in Fig. 1(a).
- Packets arrive to the output fibre according to either a Poisson process (see Section 3.1) or a 2-stage hyper-exponential process. The hyper-exponential arrival process is depicted in Fig. 1(b) and will be discussed in Section 3.2.
- The relative share of class 0 traffic is S_0, while the relative share of class 1 traffic is S_1.
- The packet lengths for both class 0 and class 1 traffic are exponential independent identical distributed (i.i.d.) with mean service time μ^{-1}.
- The system load is defined as $A = \lambda / (N \cdot \mu)$, where λ is the offered traffic intensity.
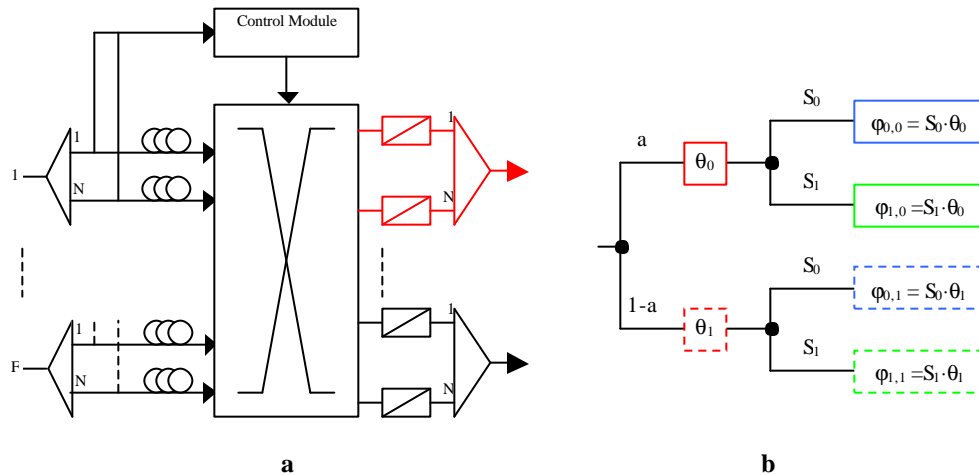- The effects of the switching time are ignored.

Fig. 1. An optical packet switch (a) and the 2-stage hyper-exponential arrival process with priorities (b).

3. The Wavelength Allocation algorithm (WA)

In order to isolate the two service classes, we utilize the WA. In the WA, a total of N available wavelengths at the output fibre are divided into two pools according to priority, i.e. a class 0 pool with W_0 wavelengths and a class 1 pool with W_1 wavelengths [6]. Incoming packets to the output fibre can access these wavelengths only if they have the necessary priority level. This means that class 1 traffic can access wavelengths only from the class 1 pool (total of $n = W_1$ wavelengths), while class 0 traffic can access wavelengths from both pools (total $N = W_1 + W_0$ wavelengths). Incoming packets which fails to acquire a wavelength is immediately dropped at the node. By adjusting the variable n, we achieve any desired level of the PLR for class 0 traffic.

3.1 Poisson arrival process

In the case of Poisson arrival process, the output fibre is modeled according to a modified M/M/N/N queuing model. Explicit results for the PLRs have been derived in earlier works (see [5]), and will not be detailed any further in this paper.

3.2 Two-stage hyper-exponential arrival process

We now turn our attention to a 2-stage hyper-exponential (H_2) arrival process with parameters a, θ_0 and θ_1, as seen in Fig. 1(b) [8]. Due to the memory-less property of the exponential

distribution, the H_2 arrival process is not long range dependent, but still bursty. We see from Fig. 1(b) that there is a probability a that the intensity of the next inter-arrival time is θ_0 (marked red) and a probability $1\text{-}a$ that the intensity of the next inter-arrival time is θ_1 (marked dotted red). We denote these arrivals as type 0 and type 1 arrivals, respectively. Furthermore, regardless of the arrival type, we see that the probability for a class 0 (blue) and class 1 (green) arrival is S_0 and S_1, respectively. Hence, the intensity of a type k arrival with priority 1 ($k, l = 0,1$) is $\varphi_{l,k}$. We also see that $\boldsymbol{q}_i = \boldsymbol{j}_{0i} + \boldsymbol{j}_{1i}$ ($i = 0,1$). The burstiness of this process can be characterized according to the squared coefficient of variation, given as [9,12]:

$$c^2 = \left(\frac{\boldsymbol{s}}{m_1}\right)^2 = \frac{m_2}{m_1^2} - 1 = \boldsymbol{e} - 1 = 2 \cdot \frac{a + k^2 - a \cdot k^2}{\left(a + k - a \cdot k\right)^2} - 1 \qquad (1)$$

Here, m_i is the i'th moment of the H_2 process, σ is the variance, ε is Palms form factor [12] and $k = \boldsymbol{q}_0 / \boldsymbol{q}_1$.
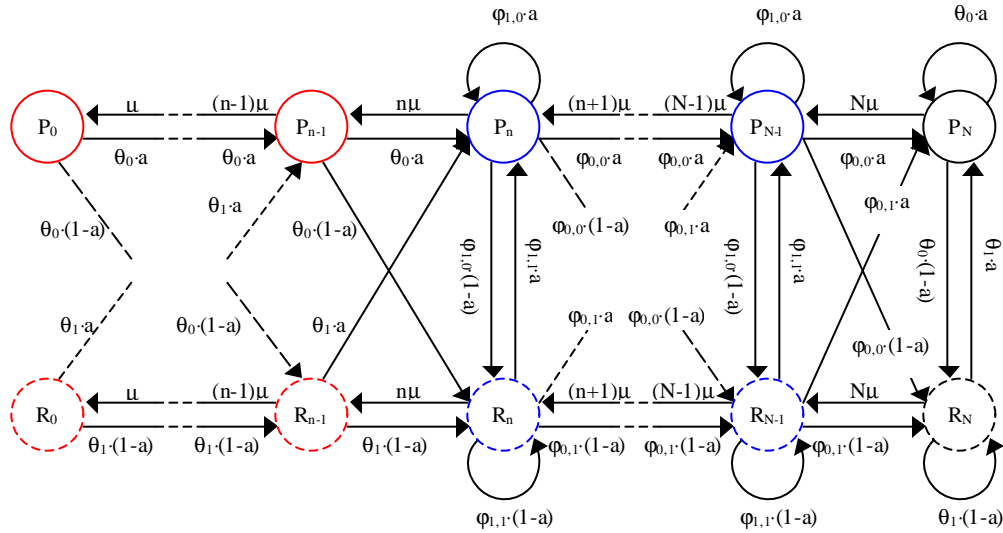

Fig. 2. Time continuous Markov chain of the WA with H_2-arrival process.

Figure 2 shows a time-continuous Markov chain of the WA with H_2-arrival process. The states P_i and R_i ($0 \leq i \leq N$) denote the number of packets currently in transmission at the output fibre, e.g. in state P_i, i packets are currently in transmission. We define p_i and r_i as the state probabilities for being in state P_i and R_i, respectively. In the P_i states (not dotted), the next arrival is a type 0 arrival, while in the R_i states (dotted) the next arrival is a type 1 arrival. Furthermore, regardless of state, we see from Fig. 2 that the probability to end in state P_i ($0 \leq i \leq N$) equals a, i.e. the probability that the next arrival is a type 0 arrival. On the opposite, the probability to end up in state R_i ($0 \leq i \leq N$) is 1-a, which is in accordance with the model in Fig. 1(b). Furthermore, in the blue and black states, only class 0 traffic is accepted. Hence, in the case of a class 1 arrival, the number of packets currently in transmission does not change, although the arrival type of the next arrival may change. In the black states, both class 0 and class 1 traffic is discarded. From Fig. 2 we can easily derive the node equations as follows:

$$p_0 \cdot \boldsymbol{q}_0 = p_1 \cdot \boldsymbol{m}, \; r_0 \cdot \boldsymbol{q}_1 = r_1 \cdot \boldsymbol{m} \qquad (2)$$

$$p_i \cdot \left(i \cdot \boldsymbol{m} + \boldsymbol{q}_0\right) = a \cdot \left(p_{i-1} \cdot \boldsymbol{q}_0 + r_{i-1} \cdot \boldsymbol{q}_1\right) + p_{i+1} \cdot \left(i+1\right) \cdot \boldsymbol{m} \quad 1 \leq i \leq n-1 \qquad (3)$$

$$p_n \cdot \left(n \cdot \boldsymbol{m} + \boldsymbol{q}_0\right) = a \cdot \left(p_{n-1} \cdot \boldsymbol{q}_0 + p_n \cdot \boldsymbol{j}_{1,0} + r_{n-1} \cdot \boldsymbol{q}_1 + r_n \cdot \boldsymbol{j}_{1,1}\right) + p_{n+1} \cdot \left(n+1\right) \cdot \boldsymbol{m} \qquad (4)$$

$$p_i \cdot (i \cdot \mathbf{m} + \mathbf{q_0}) = a \cdot \left(p_{i-1} \cdot \mathbf{j}_{0,0} + p_i \cdot \mathbf{j}_{1,0} + r_{i-1} \cdot \mathbf{j}_{0,1} + r_i \cdot \mathbf{j}_{1,1} \right) \qquad n+1 \leq i \leq N-1 \qquad (5)$$
$$+ p_{i+1} \cdot (i+1) \cdot \mathbf{m}$$

$$p_N \cdot \mathbf{q_0} = a \cdot \left(p_{N-1} \cdot \mathbf{j}_{0,0} + p_N \cdot \mathbf{q_0} + r_{N-1} \cdot \mathbf{j}_{0,1} + r_N \cdot \mathbf{q_1} \right) \qquad (6)$$

$$r_i \cdot (i \cdot \mathbf{m} + \mathbf{q_1}) = (1-a) \cdot \left(r_{i-1} \cdot \mathbf{q_1} + p_{i-1} \cdot \mathbf{q_0} \right) + r_{i+1} \cdot (i+1) \cdot \mathbf{m} \quad 1 \leq i \leq n-1 \qquad (7)$$

$$r_n \cdot (n \cdot \mathbf{m} + \mathbf{q_1}) = (1-a) \cdot \left(r_{n-1} \cdot \mathbf{q_1} + r_n \cdot \mathbf{j}_{1,1} + p_{n-1} \cdot \mathbf{q_0} + r_n \cdot \mathbf{j}_{1,0} \right) + r_{n+1} \cdot (n+1) \cdot \mathbf{m} \qquad (8)$$

$$r_i \cdot (i \cdot \mathbf{m} + \mathbf{q_1}) = (1-a) \cdot \left(r_{i-1} \cdot \mathbf{j}_{0,1} + r_i \cdot \mathbf{j}_{1,1} + p_{i-1} \cdot \mathbf{j}_{0,0} + p_i \cdot \mathbf{j}_{1,0} \right) \qquad n+1 \leq i \leq N-1 \qquad (9)$$
$$+ r_{i+1} \cdot (i+1) \cdot \mathbf{m}$$

$$r_N \cdot \mathbf{q_1} = (1-a) \cdot \left(r_{N-1} \cdot \mathbf{j}_{0,1} + r_N \cdot \mathbf{q_1} + p_{N-1} \cdot \mathbf{j}_{0,0} + p_N \cdot \mathbf{q_0} \right) \qquad (10)$$

$$\sum_{i=0}^{N} p_i + \sum_{i=0}^{N} r_i = 1 \qquad (11)$$

The PLR for class 0 traffic equals the number of lost class 0 arrivals divided by the total number of class 0 arrivals. We know that class 0 arrivals are discarded only in states P_N and R_N (black states). In state P_N the arrival intensity for class 0 traffic is $\varphi_{0,0}$, while in state R_N the arrival intensity is $\varphi_{0,1}$. Class 1 traffic is lost in the states $\{P_n,\ldots,P_N\}$ and $\{R_n,\ldots,R_N\}$ (blue and black states). This leads us to the PLR for class 0 ($P_{H_2}^0$) and class 1 ($P_{H_2}^1$) traffic in Eq. (12). At last, the average PLR is given in Eq. (13).

$$P_{H_2}^0 = \frac{p_N \cdot \mathbf{j}_{0,0} + r_N \cdot \mathbf{j}_{0,1}}{\mathbf{j}_{0,0} \cdot \sum_{i=0}^{N} p_i + \mathbf{j}_{0,1} \cdot \sum_{i=0}^{N} r_i}, \qquad P_{H_2}^1 = \frac{\mathbf{j}_{1,0} \cdot \sum_{i=n}^{N} p_i + \mathbf{j}_{1,1} \cdot \sum_{i=n}^{N} r_i}{\mathbf{j}_{1,0} \cdot \sum_{i=0}^{N} p_i + \mathbf{j}_{1,1} \cdot \sum_{i=0}^{N} r_i} \qquad (12)$$

$$P_{H_2}^{av} = \frac{p_N \cdot \mathbf{q_0} + r_N \cdot \mathbf{q_1} + \mathbf{j}_{1,0} \cdot \sum_{i=n}^{N-1} p_i + \mathbf{j}_{1,1} \cdot \sum_{i=n}^{N-1} r_i}{\mathbf{q_0} \cdot \sum_{i=0}^{N} p_i + \mathbf{q_1} \cdot \sum_{i=0}^{N} r_i} \qquad (13)$$

4. Results

For the rest of the paper, unless stated differently, we have used N = 4 wavelengths, C = 2,5 Gbps, A = 0,4, S_0 = 0,2 and n = 3. The mean packet length equals 472 bytes, which means that the mean duration of a packet is μ^{-1} = 1,5104 µs. Several simulation runs have been performed until the desired level of confidence has been achieved. First, simulations have been performed in order to verify the analytical model presented in Section 3.2. Regarding the arrival process, we have used a = 0,2 and θ_0 = 50θ_1. The results can be seen in Table 1.

Table 1. Simulation and analytical results.

System load	0,2	0,4	0,6	0,8	1,0
Analytical class 0	$6,559 \cdot 10^{-3}$	$2,379 \cdot 10^{-2}$	$4,783 \cdot 10^{-2}$	$7,499 \cdot 10^{-2}$	$1,030 \cdot 10^{-1}$
Simulation class 0	$6,452 \cdot 10^{-3}$	$2,376 \cdot 10^{-2}$	$4,793 \cdot 10^{-2}$	$7,476 \cdot 10^{-2}$	$1,030 \cdot 10^{-1}$
95% conf. limits	$\pm 1,413 \cdot 10^{-4}$	$\pm 1,636 \cdot 10^{-4}$	$\pm 2,116 \cdot 10^{-4}$	$\pm 2,177 \cdot 10^{-4}$	$\pm 1,613 \cdot 10^{-4}$
Analytical class 1	$8,737 \cdot 10^{-2}$	$2,154 \cdot 10^{-1}$	$3,374 \cdot 10^{-1}$	$4,394 \cdot 10^{-1}$	$5,217 \cdot 10^{-1}$
Simulation class 1	$8,727 \cdot 10^{-2}$	$2,154 \cdot 10^{-1}$	$3,374 \cdot 10^{-1}$	$4,393 \cdot 10^{-1}$	$5,217 \cdot 10^{-1}$
95% conf. limits	$\pm 2,415 \cdot 10^{-4}$	$\pm 2,663 \cdot 10^{-4}$	$\pm 2,544 \cdot 10^{-4}$	$\pm 1,823 \cdot 10^{-4}$	$\pm 1,739 \cdot 10^{-4}$

From Table 1 we see that the simulation results matches the analytical results closely, which means that the proposed analytical model is very accurate. This is an improvement compared

to the analytical models proposed in [9], which are very inaccurate, especially in the case of low system loads. Further in the paper, in order to determine the variables for the H_2 arrival process, we have utilized the balanced mean fit distribution and the gamma fit distribution [9]. The parameters for the balanced mean fit distribution are seen in Eq. (14), and the parameters for the gamma fit distribution are seen in Eq. (15).

$$a = \left(1 + \sqrt{(c^2 - 1)/(c^2 + 1)}\right)\Big/ 2, \; \mathbf{q}_0 = 2 \cdot a \cdot \mathbf{l}, \; \mathbf{q}_1 = 2 \cdot \mathbf{l} \cdot (1 - a) \tag{14}$$

$$\mathbf{q}_0 = 2 \cdot \mathbf{l} \cdot \left(1 + \sqrt{(c^2 - 1/2)/(c^2 + 1)}\right), \; \mathbf{q}_1 = 4 \cdot \mathbf{l} - \mathbf{q}_0, \; a = \left(\mathbf{q}_0 (\mathbf{q}_1 / \mathbf{l} - 1)\right)\Big/(\mathbf{q}_1 - \mathbf{q}_0) \tag{15}$$
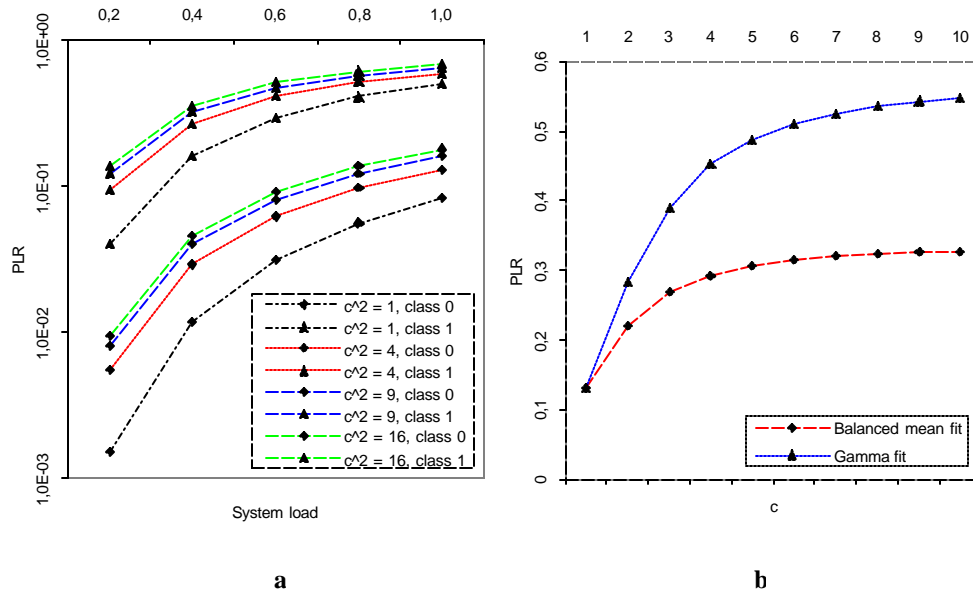

Fig. 3. The PLR as a function of the system load (a) and the average PLR as a function of the coefficient of variation (b).

Figure 3(a) shows the PLR as a function of the system load for different values of the squared coefficient of variation (c^2). Here, we have utilized the balanced mean fit distribution. First, regardless of traffic -class, we see that the PLR increases when c^2 increases. This is expected since an increase in c^2 means that the traffic is increasingly bursty. Furthermore, we see that the difference in the PLR decreases as a function of an increasing system load. This is because at high loads, packet losses are dominated by congestion caused by high system load and not bursty traffic. Figure 3(b) shows the PLR as a function of the coefficient of variation for the balanced mean fit and the gamma fit distribution. First, we see that the balanced mean fit distribution show better performance compared to the gamma fit distribution. Second, we see that the increase in the PLR decreases when the coefficient of variation increases, which means that increasing the burstiness has greater impact on the PLR when the arrival process is initially less bursty.

5. Conclusion

This paper presented an analytical model of a service differentiated bufferless OPS network with a bursty hyper-exponential arrival process. Although not as general as the models proposed in [9], the proposed model is more accurate, especially at low system loads (i.e. A < 0,8). Results obtained from the model indicate that the PLR increases as the burstiness of the arrival process increases, which is in accordance with results from previous research [4,9].